

# External magnetic fields and the chiral phase transition in QED at nonzero chemical potential

W.-C. Syu, D.-S. Lee

*Department of Physics, National Dong Hwa University,  
Shoufeng, Hualien 974, Taiwan, R.O.C.*

C. N. Leung

*Department of Physics and Astronomy,  
University of Delaware, Newark, DE 19716, U.S.A.*

(Dated: November 25, 2021)

## Abstract

Inspired by recent discussions of inverse magnetic catalysis in the literature, we examine the effects of a uniform external magnetic field on the chiral phase transition in quenched ladder QED at nonzero chemical potential. In particular, we study the behaviour of the effective potential as the strength of the magnetic field is varied while the chemical potential is held constant. For a certain range of the magnetic field, the effective potential develops a local maximum. Inverse magnetic catalysis is observed at this maximum, whereas the usual magnetic catalysis is observed at the true minimum of the effective potential.

PACS numbers:

The effect of external fields on the symmetry properties of the vacuum has been extensively studied in the past decades. Under the quenched, ladder approximation of QED, chiral symmetry is dynamically broken at weak gauge couplings when a uniform magnetic field is present [1, 2]. The dynamically generated fermion mass is obtained that increases with growing magnetic field strength. The phenomenon is referred to as magnetic catalysis of chiral symmetry breaking. A subsequent analysis [3] shows that an improved truncation beyond the quenched ladder approximation produces a gauge independent dynamical fermion mass within the lowest Landau level approximation, provided that it is obtained from the fermion self-energy evaluated on shell.

Recent lattice studies of hot QCD in an external (electro)magnetic field found that the critical temperature of the chiral phase transition decreases with increasing magnetic field [4], contrary to the expectation from magnetic catalysis. This is known as inverse magnetic catalysis. Although there are several proposed ideas for explaining this unexpected behaviour [5], what causes this anomalous phenomenon remains an open question. Recent field theoretic studies did not arrive at a definite conclusion about how the critical chemical potential for the chiral phase transition vary with the strength of the external magnetic field [6].

Previous works on quenched ladder QED in an external magnetic field show that chiral symmetry is restored above a certain critical value of temperature [7–9] as well as critical chemical potential [9]. Since the critical temperature and chemical potential are measured in units of  $\sqrt{|eH|}$ , where  $H$  is the magnetic field, it suggests that their values will increase with increasing magnetic field and the system does not exhibit behaviour of inverse magnetic catalysis. Prompted by the current interest in inverse magnetic catalysis, we reexamine these earlier works more carefully to determine the effects of the magnetic field on the chiral phase transition. We shall focus on the effects on the critical chemical potential in this paper.

We employ the effective potential approach of Ref. [10], with modifications relevant to studying the chiral dynamics in the case of nonzero chemical potential. The detailed profile of the effective potential and the location of its extrema will enable one to construct the phase diagram of the chiral dynamics and understand the nature of the phase transition.

We begin by constructing the effective potential for chiral dynamics in terms of the expectation value of composite local fields,  $\sigma(x) = \langle 0 | \bar{\psi}(x) \psi(x) | 0 \rangle$  and  $\pi(x) = \langle 0 | \bar{\psi}(x) i \gamma_5 \psi(x) | 0 \rangle$ . To do so, consider the generating functional

$$\begin{aligned} Z[J_\sigma, J_\pi] &\equiv \exp(iW[J_\sigma, J_\pi]) \\ &= \int \mathcal{D}\psi(x) \mathcal{D}\bar{\psi}(x) \mathcal{D}A_\mu(x) \cdot \\ &\quad \exp\left(i \int d^4x \left[ \mathcal{L} + J_\sigma(x) \bar{\psi}(x) \psi(x) + J_\pi(x) \bar{\psi}(x) i \gamma_5 \psi(x) \right]\right), \end{aligned} \quad (1)$$

where  $\mathcal{L}$  is the Lagrangian density of massless QED in a uniform external magnetic field pointing in the  $z$  direction. The expectation values of the composite fields can be obtained by taking the usual variation of the generating functional with respect to the sources:

$$\frac{\delta W}{\delta J_\sigma(x)} = \sigma(x), \quad \frac{\delta W}{\delta J_\pi(x)} = \pi(x). \quad (2)$$

By inverting the expressions (2) to write  $\sigma$  and  $\pi$  as a function of the sources, the effective action can be obtained through the Legendre transformation

$$\Gamma[\sigma, \pi] = W[J_\sigma, J_\pi] - \int d^4x [J_\sigma(x)\sigma(x) + J_\pi(x)\pi(x)], \quad (3)$$

from which

$$\frac{\delta\Gamma}{\delta\sigma(x)} = -J_\sigma(x), \quad \frac{\delta\Gamma}{\delta\pi(x)} = -J_\pi(x). \quad (4)$$

For spacetime independent fields,  $\sigma_0$  and  $\pi_0$  are given by the corresponding constant sources  $j_\sigma$  and  $j_\pi$ , respectively. The effective potential is found to be

$$V[\sigma_0, \pi_0] = -\frac{1}{\Omega}\Gamma[\sigma_0, \pi_0], \quad (5)$$

where  $\Omega$  is the spacetime volume. The presence of chiral symmetry renders the effective action/potential a function of  $\rho = (\sigma^2 + \pi^2)^{1/2}$  only. It is thus sufficient and convenient to simply consider, e.g., the case  $\pi = 0$  and  $\sigma \neq 0$ . The complete functional form of the effective potential can be found via substituting  $\sigma_0 = \rho$ . In terms of the spacetime independent generating functional, denoted by  $w[j] = W[j]/\Omega$ , where we have simplified the notation by setting  $j_\sigma = j$ , the effective potential now becomes

$$V[\rho] = j\rho - w[j], \quad (6)$$

where

$$w[j] = \int \rho dj. \quad (7)$$

Applying the above to the case of nonzero chemical potential and using the quenched ladder approximation that takes into account contributions from the lowest Landau level only, we find

$$j \simeq -m_\mu + \frac{\alpha}{2\pi}|eH|m_\mu \int_{-\infty}^{\infty} dq_3 \int_0^{\infty} d\hat{q}_\perp^2 \frac{e^{-\hat{q}_\perp^2}}{Q_1 Q_2} \cdot [f_+(Q_1, Q_2) + \theta(Q_1 - \mu)f_-(Q_1, Q_2) + \theta(\mu - Q_1)f_-(Q_1, -Q_2)], \quad (8)$$

where  $\hat{q}_\perp^2 \equiv (q_1^2 + q_2^2)/(2|eH|)$ ,  $Q_1^2 \equiv q_3^2 + m_\mu^2$ ,  $Q_2^2 \equiv q_3^2 + 2|eH|\hat{q}_\perp^2$ ,  $\alpha$  is the fine structure constant, and  $m_\mu$  is the infrared dynamical fermion mass which is a function of the chemical potential  $\mu$  ( $\mu \equiv |\mu| > 0$ ) and the external source  $j$  [7, 9]. The functions  $f_\pm$  are defined as

$$f_\pm(Q_1, Q_2) = \frac{1}{Q_1 + Q_2 \pm \mu}. \quad (9)$$

The chiral condensate,  $\rho = \langle \bar{\psi}\psi \rangle_\mu$ , is found to be

$$\rho \simeq -\frac{|eH|}{\pi^2}m_\mu \left[ \theta(m_\mu - \mu) \int_0^{\sqrt{|eH|}} \frac{dq_3}{\sqrt{q_3^2 + m_\mu^2}} + \theta(\mu - m_\mu) \int_{\sqrt{\mu^2 - m_\mu^2}}^{\sqrt{|eH|}} \frac{dq_3}{\sqrt{q_3^2 + m_\mu^2}} \right]. \quad (10)$$

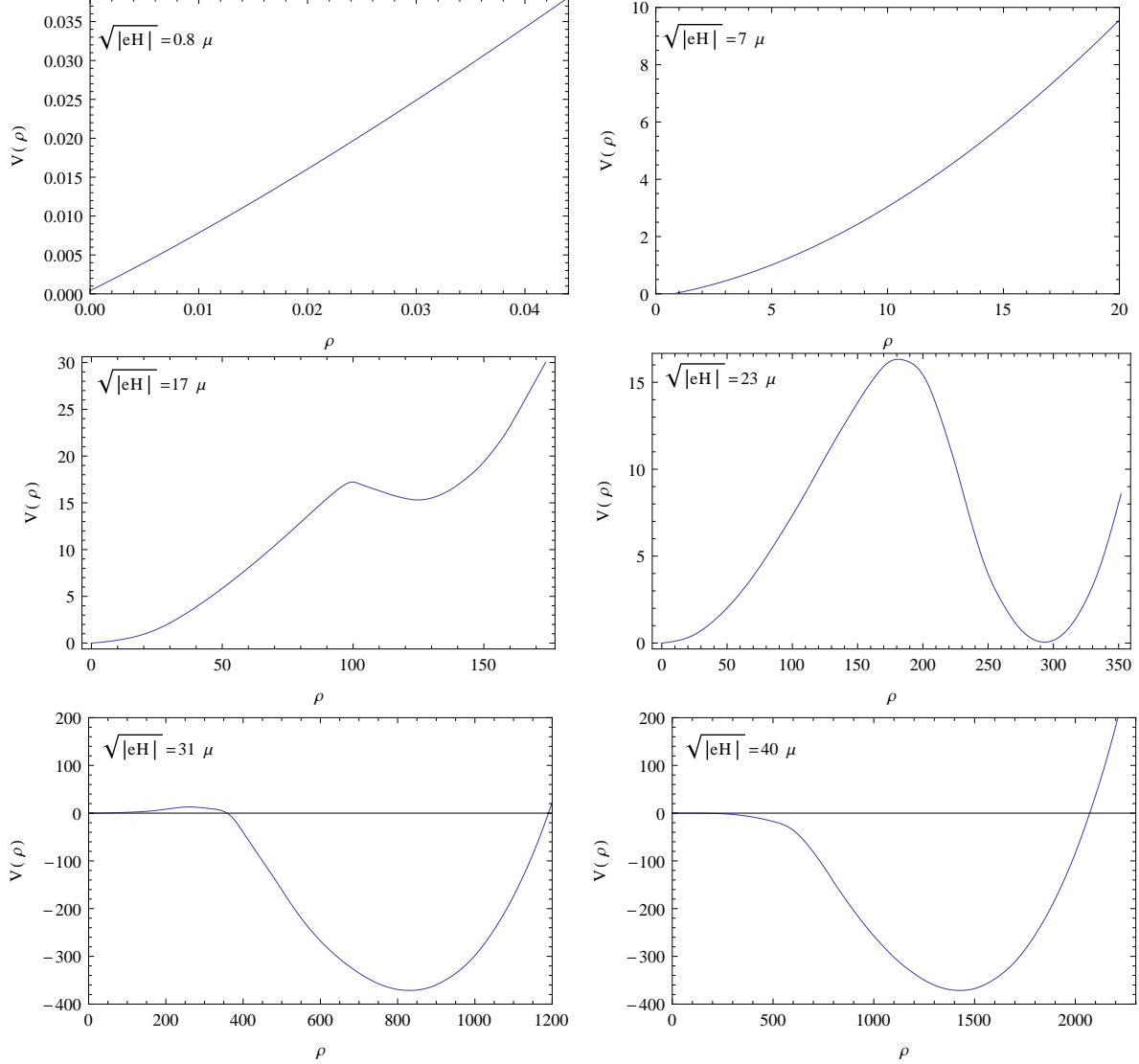


FIG. 1: The effective potential as a function of the chiral condensate for different values of the magnetic field strength. Both  $V$  and  $\rho$  are measured in units of  $\mu$ , the constant chemical potential.  $\alpha = \pi/10$  for all graphs.

The effective potential  $V(\rho)$  is evaluated numerically for various values of the magnetic field in units of the chemical potential  $\mu$ . Some sample results are shown in Fig.1. It is found that, for  $\sqrt{|eH|} \leq \mu$ , the effective potential has only one minimum, which is located at  $\rho = 0$ , corresponding to the chirally symmetric phase. See the first graph in Fig.1. For  $\sqrt{|eH|} > \mu$ , the second and third graphs in Fig.1 show that, as the magnetic field is increased, the effective potential starts to develop two additional local extrema, a local minimum and a local maximum, at nonzero values of  $\rho$ . The global minimum at  $\rho = 0$  preserves chiral symmetry. As the magnetic field reaches a certain strength, the two minima become degenerate and a first-order phase transition is about to occur (see the fourth graph in Fig.1). When the field strength is above this critical value, the global minimum of  $V(\rho)$  is shifted to a nonzero value of  $\rho$  and chiral symmetry is spontaneously broken. In particular, the expectation value  $\rho$  at the global minimum increases with the increase in the magnetic

field, consistent with the expectation of magnetic catalysis (see the last two graphs in Fig.1). On the contrary, as the strength of the magnetic field increases, the expectation value at the local maximum, the unstable state, increases and then shifts toward  $\rho = 0$ . This gives rise to the anomalous inverse magnetic catalysis effect and is shown in Fig.2. In Fig.3, the corresponding dynamical mass for the ground state and the unstable state is also shown. Again the unstable state exhibits features of inverse magnetic catalysis. These figures show again that the magnetic field must exceed a certain critical value for spontaneous chiral symmetry breaking to take place when the chemical potential is not zero.

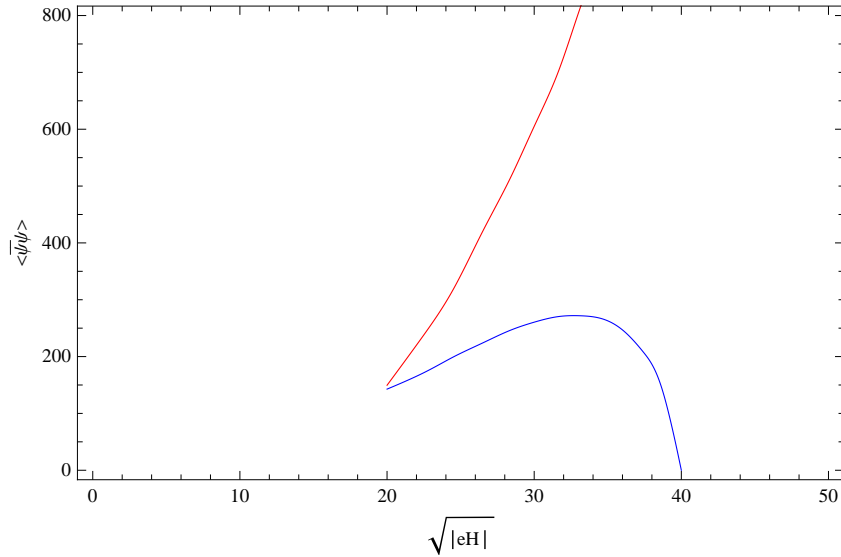


FIG. 2: The fermion condensate, in units of  $\mu^3$ , as a function of the magnetic field ( $\sqrt{|eH|}$  in units of  $\mu$ ) for  $\alpha = \pi/10$ . The red curve corresponds to the global minimum of the effective potential and behaves as expected from magnetic catalysis, whereas the blue curve for the local maximum of the effective potential exhibits inverse magnetic catalysis behaviour.

To better understand the numerical results above, let us examine the behaviour of the effective potential more closely. For  $m_\mu < \mu$ , the behavior of the effective potential can be found by first obtaining the corresponding approximate expression of (8) for small  $m_\mu$ ,

$$j \simeq c_1 m_\mu + c_3 m_\mu^3 + \mathcal{O}(m_\mu^5), \quad (11)$$

where the constants  $c_1$  and  $c_3$  depend on the chemical potential and the magnetic field. Specifically,

$$\begin{aligned} c_1(H, \mu) &= -1 + \frac{\alpha}{2\pi} |eH| \int_{-\infty}^{\infty} dq_3 \int_0^{\infty} d\hat{q}_\perp^2 \frac{e^{-\hat{q}_\perp^2}}{q_3 Q_2} \cdot \\ &\quad [f_+(q_3, Q_2) + \theta(q_3 - \mu) f_-(q_3, Q_2) + \theta(\mu - q_3) f_-(q_3, -Q_2)], \\ c_3(H, \mu) &= \frac{\alpha}{\pi} \frac{|eH|}{\mu^2} \int_0^{\infty} d\hat{q}_\perp^2 \frac{e^{-\hat{q}_\perp^2}}{2|eH|\hat{q}_\perp^2 + \mu^2}. \end{aligned} \quad (12)$$

A nontrivial approximate solution for the gap equation can be obtained by setting the source  $j$  equal to zero, yielding

$$m_{\mu 0; \text{unstable}} \simeq \sqrt{-c_1/c_3}. \quad (13)$$

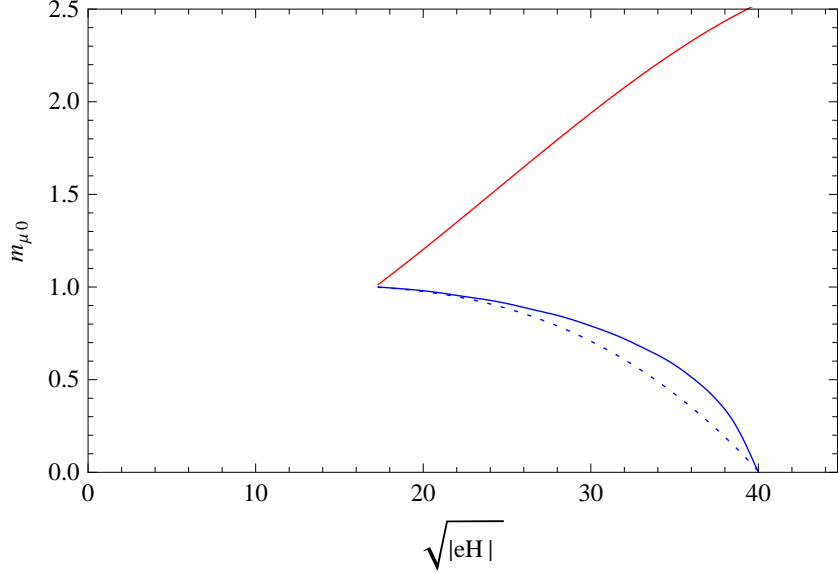


FIG. 3: The dynamical fermion mass (in units of  $\mu$ ) as a function of the magnetic field for  $\alpha = \pi/10$ . The red curve corresponds to the global minimum of the effective potential and behaves as expected from magnetic catalysis, whereas the blue curve for the local maximum of the effective potential exhibits inverse magnetic catalysis behaviour. For comparison, the approximate result for  $m_{\mu 0; \text{unstable}}$  from Eq. (13) is shown by the dotted curve.

Note that  $c_3$  is always positive and  $c_1$  is negative for some range of the parameters. It can be seen from Fig.3 that this solution, which is valid for  $m_\mu < \mu$ , corresponds to the unstable local maximum of the effective potential. We also plotted in Fig.3 this approximate result for  $m_{\mu 0; \text{unstable}}$  to compare with the exact numerical result. A reasonably good agreement is found. The decrease of  $m_{\mu 0; \text{unstable}}$  with increasing magnetic field can be understood by observing that, for a larger value of the magnetic field,  $c_1$  is less negative whereas  $c_3$  is larger.

Turning now to the behaviour of the chiral condensate  $\rho$  for small  $m_\mu$ , we find from Eq. (10) that

$$\rho \simeq -\frac{|eH|}{\pi^2} m_\mu \ln \left[ \left( \sqrt{|eH|} + \sqrt{|eH| + m_\mu^2} \right) / \left( \mu + \sqrt{\mu^2 - m_\mu^2} \right) \right]. \quad (14)$$

Using the approximate expressions for  $j$  and  $\rho$  above, one finds from Eq. (7) that, for  $m_\mu < \mu$ ,

$$\begin{aligned} w_{<} &= \int_0^{m_\mu} \rho(m) \frac{dj}{dm} dm \\ &\simeq -\frac{|eH|}{2\pi^2} \ln \left( \sqrt{|eH|}/\mu \right) \left( c_1 m_\mu^2 + \frac{3c_3}{2} m_\mu^4 \right) - \frac{c_1}{16\pi^2} \left[ 1 + \frac{|eH|}{\mu^2} \right] m_\mu^4 + \mathcal{O}(m_\mu^6). \end{aligned} \quad (15)$$

It follows from Eq. (6) that the corresponding effective potential is

$$\begin{aligned} V_{<} \simeq & -\frac{c_1}{2\pi^2} |eH| \ln \left( \sqrt{|eH|}/\mu \right) m_\mu^2 - \left[ \frac{3c_1}{16\pi^2} \left( 1 + \frac{|eH|}{\mu^2} \right) \right. \\ & \left. + \frac{c_3}{4\pi^2} |eH| \ln \left( \sqrt{|eH|}/\mu \right) \right] m_\mu^4 + \mathcal{O}(m_\mu^6). \end{aligned} \quad (16)$$

This approximation is compared with the numerical result for the full effective potential in Fig.4. It is seen to give a reliable description for  $m_\mu < 0.5\mu$ . We check that, for sufficiently large magnetic field, the term proportional to  $c_3$  in the coefficient of the  $m_\mu^4$  dominates, thus reproducing the solution (13). The result of (16) also indicates that the unstable local maximum of the effective potential starts to develop when  $\sqrt{|eH|} > \mu$  and  $c_1 < 0$ , leading to a positive coefficient for the  $m_\mu^2$  term and negative coefficient for the  $m_\mu^4$  term, and then disappears when  $c_1$  turns positive as the magnetic field exceeds certain critical value, consistent with our numerical finding in Fig.1.

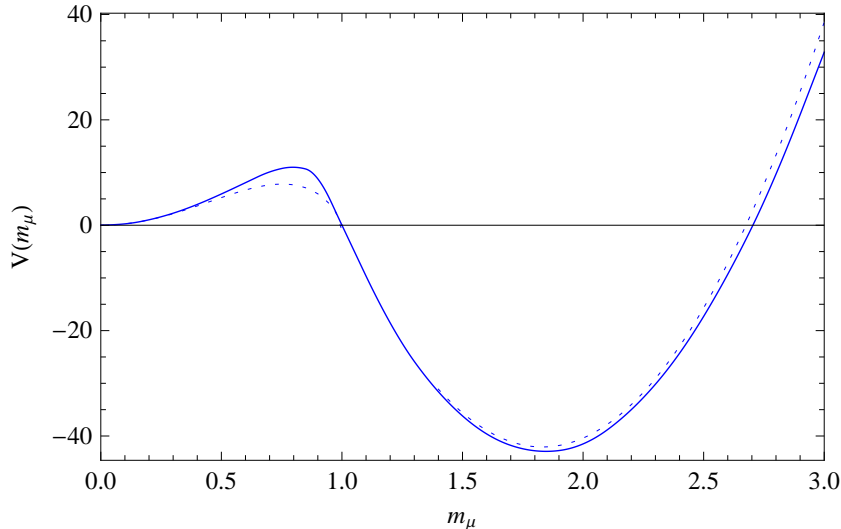


FIG. 4: Comparison of the full (solid) and the approximate (dotted) effective potentials for  $\alpha = \pi/10$  and  $\sqrt{|eH|} = 28.3 \mu$ . Both  $V$  and  $m_\mu$  are measured in units of  $\mu$ .

We perform a similar analysis for the case  $m_\mu > \mu$ . Specifically we examine the behaviour of the effective potential in the neighbourhood of  $m_\mu = m_{\mu 0}$ , the ground-state solution of the gap equation. We find approximate expressions for

$$j \simeq b_1 (m_\mu - m_{\mu 0}) + b_2 (m_\mu - m_{\mu 0})^2 + \mathcal{O}(m_\mu - m_{\mu 0})^3 \quad (17)$$

and

$$\rho \simeq -\frac{|eH|}{\pi^2} m_\mu \ln \left[ (\sqrt{|eH|} + \sqrt{|eH| + m_\mu^2}) / m_\mu \right], \quad (18)$$

from which we obtain the effective potential in the form

$$V_{>} \simeq v_0 + v_2 (m_\mu - m_{\mu 0})^2 + \mathcal{O}(m_\mu - m_{\mu 0})^3. \quad (19)$$

The detailed expressions for the coefficients  $b_1$ ,  $b_2$ ,  $v_0$ , and  $v_2$  are not very illuminating. Instead, we show the result in Fig.4 and compare it with the full effective potential. The agreement is quite good and the global minimum of the effective potential is correctly produced. As shown in Figs.2 and 3, this true vacuum behaves like what one would expect from magnetic catalysis as the magnetic field is varied.

In summary, we have reexamined the effect of an external magnetic field on the chiral phase transition in QED at a finite chemical potential through the effective potential of order parameter fields relevant to the chiral dynamics. We observe differing behaviour between the true vacuum (global minimum of the effective potential) and the unstable local maximum of the effective potential. While both are solutions to the gap equation, the true vacuum behaves according to magnetic catalysis while the solution at the local maximum behaves according to inverse magnetic catalysis. Since the chiral phase transition is governed by the vacuum solution, we conclude that quenched ladder QED at nonzero chemical potential exhibits characteristics of magnetic catalysis. It is useful and interesting to also include thermal fluctuations in this study. Work along this direction is in progress.

### Acknowledgments

The work of DSL was supported in part by the National Science Council of Taiwan. Part of the work of CNL was carried out while he was visiting the Academia Sinica and National Dong Hwa University in Taiwan. He thanks these institutions for their support and hospitality.

- 
- [1] V. P. Gusynin, V. A. Miransky, and I. A. Shovkovy, Phys. Rev. D **52**, 4747 (1995); Nucl. Phys. **B462**, 249 (1996).
  - [2] C. N. Leung, Y. J. Ng, and A. W. Ackley, Phys. Rev. D **54**, 4181 (1996).
  - [3] C. N. Leung and S.-Y. Wang, Nucl. Phys. B **747**, 266 (2006); Annals Phys. **322**, 701 (2007).
  - [4] G.S. Bali *et al*, JHEP **1202**, 044 (2012); PoS **LATTICE2011**, 192 (2011); Phys. Rev. D **86**, 071502 (2012); G. S. Bali, PoS **ConfinementX**, 198 (2012).
  - [5] K. Fukushima and Y. Hidaka, Phys. Rev. Lett. **110**, 031601 (2013); T. Kojo and N. Su, Phys. Lett. B **720**, 192 (2013); F. Bruckmann, G. Endrodi and T. G. Kovacs, JHEP **1304**, 112 (2013); J. Chao, P. Chu and M. Huang, arXiv:1305.1100 [hep-ph].
  - [6] F. Preis, A. Rebhan and A. Schmitt, JHEP **1103**, 033 (2011); AIP Conf. Proc. **1492**, 264 (2012); A.F. Garcia and M.B. Pinto, arXiv:1307.2451 [hep-ph]; P.G. Allen and N.N. Scoccola, arXiv:1307.4070 [hep-ph].
  - [7] D.-S. Lee, C. N. Leung and Y. J. Ng, Phys. Rev. D **55**, 6504 (1997).
  - [8] V. P. Gusynin and I. A. Shovkovy, Phys. Rev. D **56**, 5251 (1997).
  - [9] D.-S. Lee, C. N. Leung and Y. J. Ng, Phys. Rev. D **57**, 5224 (1998).
  - [10] D.-S. Lee, P. N. McGraw, Y. J. Ng, and I. A. Shovkovy, Rev. D **59**, 085008 (1999).